Available online at www.sciencedirect.com

ScienceDirect

IFAC PapersOnline CONFERENCE PAPER ARCHIVE

IFAC PapersOnLine 55-31 (2022) 166–171

Control Considerations for Very Large Floating Wind Turbines ⋆

Carlos Renan dos Santos * **Serag-Eldin Abdelmoteleb** **
Alejandra S. Escalera Mendoza ***
Erin E. Bachynski-Polić ****

* *Institute for Energy Technology, 2007 Kjeller, Norway (e-mail: carlos.santos@ife.no).*
** *Norwegian University of Science and Technology, 7491 Trondheim, Norway (e-mail: serageldin.abdelmoteleb@ntnu.no)*
*** *The University at Texas at Dallas, Richardson, Texas, 75080-3021, USA, (e-mail: Alejandra.EscaleraMendoza@UTDallas.edu)*
**** *Norwegian University of Science and Technology, 7491 Trondheim, Norway (e-mail: erin.bachynski@ntnu.no)*

Abstract: Increasingly large floating wind turbines (FWTs) are being introduced to access the offshore wind resource over deep water at lower cost. In connection with designing a 25 MW semi-submersible wind turbine, we examine the scaling trends associated with the dynamic performance of the generator torque and blade pitch controllers and highlight the challenges that may be encountered for such devices. The increased rotor inertia, reduced blade pitch rates, longer platform pitch and surge natural periods, and flexible modes of the tower, platform, and rotor all affect the ability of the controller to track the desired rotor speed. The effects of control design and tuning choices on the FWT behavior in representative wind and wave conditions are shown.

Keywords: Floating wind turbines, control design, large-scale wind turbine, floating platform, detuning approach.

1. INTRODUCTION

In an effort to harvest the wind energy resource over deep water at lower costs, there is great interest in developing increasingly large floating wind turbines. By increasing the rated power of each turbine, the levelized cost of the substructure, cabling, mooring, and maintenance can potentially be reduced. Recently, reference turbines and platforms on the order of 12-15 MW have been introduced (de Souza et al., 2021; Gaertner et al., 2020). The operational (closed-loop) generator torque and blade pitch control systems play an increasingly important role in the dynamic responses of such structures. Understanding how the control performance changes for larger turbines is necessary for designing the rotor, tower, and platform.

Larsen and Hanson (2007) observed that the application of a controller tuned for an onshore wind turbine to a floating version leads to severe instabilities. Therefore, the development of control systems for floating wind turbines constitutes a flourishing research field. As discussed in Section 2, many enhancements and adaptations have been proposed to classical PID controllers, which are extensively employed due to their simplicity and robustness (Ha et al., 2021). Floating wind turbines can also benefit from the use of individual pitch controllers to enhance their stability (Salic et al., 2019). Moreover, several authors propose the use of LIDAR measurements as a tool for the improvement of control approaches applied to floating turbines (Gottschall et al., 2017).

2. CONTROL OBJECTIVES AND TYPICAL CONTROL STRATEGIES

The closed-loop controller for a modern variable-speed, variable-pitch wind turbine has multiple, possibly conflicting objectives (Manwell et al., 2009; Bossanyi, 2003), such as:

- Maximising energy capture;
- Limiting aerodynamic loads in high winds;
- Damping out torsional resonances, e.g. in the drive train;
- Producing smooth power (power quality);
- Damping other dynamic modes (fore-aft motions, side-side motions);
- Limiting actuator activity (such as blade pitch actuation).

The most common control strategy for modern wind turbines is a variable-speed, variable-pitch approach. The simplest behavior of a wind turbine following this strategy is illustrated in Fig. 1, showing the mean rotor speed, generator torque, generator power, and blade pitch angle as a function of the mean wind speed. A few control regions are also indicated: Region 1 (below cut-in, no power is

⋆ The research leading to these results has received funding from the Research Council of Norway through the ENERGIX program (grant 308839) and industry partners Equinor, AIBEL, Dr. Techn. Olav Olsen, GCE Node Service, and Energy Valley.

10.1016/j.ifacol.2022.10.426

extracted), Region 2 (in between cut-in and rated), Region 3 (above rated wind speed, but below the cut-out wind speed), and Region 4 (beyond cut-out wind speed, the blades are fully pitched and no power is extracted).

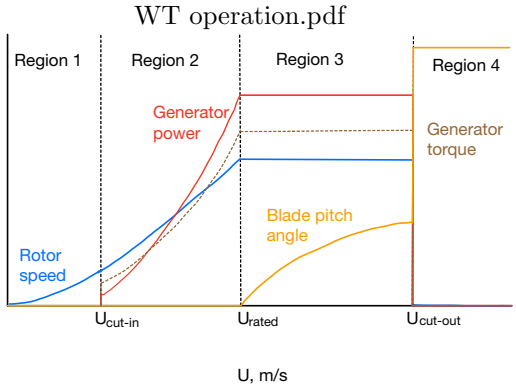

Fig. 1. Typical operational strategy of a VSVP wind turbine as a function of wind speed U.

In Region 2, the goal is to extract as much of the available energy in the wind as possible by maintaining the optimal tip speed ratio $\lambda = \omega R/U$ (where R is the rotor radius, ω is the rotor speed, and U is the wind speed), and maintaining approximately constant blade pitch. In such a strategy, the rotor speed increases approximately linearly with mean wind speed, while the generator torque increases quadratically and the generator power increases approximately cubically. The generator torque command can be found by using the quadratic relationship:

$$Q = \frac{C_p \frac{1}{2}\rho\pi R^5 \omega^2}{\lambda^3}. \tag{1}$$

where C_p is the power coefficient and ρ is the density of air. The torque controller command can be determined directly by lookup table or by a proportional-integral controller.

Beyond the rated wind speed, in Region 3, the blade pitch controller is also active (in addition to the generator torque controller). The steady-state values of the rotor speed, generator power, and generator torque do not vary with wind speed. In Region 3, the objective is no longer to extract as much power as possible from what is available in the wind, but rather to reduce the loads on the turbine while still extracting power at the rated level.

In Region 3, the generator torque is adjusted to try to maintain constant power:

$$Q_{gen} = \frac{P_{rated}}{\omega}. \tag{2}$$

where P_{rated} is the rated power. The blade pitch angle is adjusted using proportional-integral control based on the error in the rotor speed:

$$\Delta\theta = K_P \Delta\omega + K_I \int_0^t \Delta\omega(\tau) d\tau \tag{3}$$

where $\Delta\theta$ is the change in blade pitch angle, K_P and K_I are the proportional and integral gains, respectively, and $\Delta\omega$ is the rotor speed error, $\Delta\omega = \omega - \omega_{ref}$. Typically, ω_{ref} is taken as the rated rotor speed, and the measured ω is low-pass filtered with a cut-off frequency close to the blade first edgewise natural frequency. The corner frequency for this filter is placed at 0.25 Hz for the NREL 5 MW turbine (Jonkman et al., 2009), 0.2 Hz for the DTU 10 MW turbine (Bak et al., 2015), and 0.16 Hz for the IEA 15 MW turbine (Gaertner et al., 2020).

Given the control strategy in Region 3, an analysis of the rotor dynamics can be used to show that the controlled system acts as a second order system, similar to a mass-spring-dashpot (Jonkman et al., 2009):

$$I\ddot{\psi} + \left[\frac{1}{\omega_{rated}}\left(-\frac{\partial P_{aero}}{\partial\theta}\right) K_P - \frac{P_0}{\omega_{rated}^2}\right]\dot{\psi} + \left[\frac{1}{\omega_{rated}}\left(-\frac{\partial P_{aero}}{\partial\theta}\right) K_I\right]\psi = 0 \tag{4}$$

where I represents the combined inertia of the rotor and drivetrain, $-\frac{\partial P_{aero}}{\partial\theta}$ is the sensitivity of the aerodynamic power to changes in the blade pitch angle, P_0 is the rated power, ω_{rated} is the rated rotor speed, and ψ is related to the rotor azimuth. Given that the sensitivity of the aerodynamic power generally depends on the operational point, the scheduled gains can be selected to achieve a desired system natural frequency ($\omega_{0,\psi}$) and damping ratio (ζ_ψ) as:

$$K_P = \frac{2I\omega_{rated}\zeta_\psi\omega_{0,\psi}}{\left(-\frac{\partial P_{aero}}{\partial\theta}\right)}, \tag{5}$$

$$K_I = \frac{I\omega_{rated}\omega_{0,\psi}^2}{\left(-\frac{\partial P_{aero}}{\partial\theta}\right)}. \tag{6}$$

For land-based or bottom-fixed wind turbines, $\omega_{0,\psi}$ is often chosen to be approximately 0.6 rad/s (corresponding to a period of approximately 10 s) (Jonkman et al., 2009; Jonkman, 2010). For floating wind turbines, there are concerns related to the possibility of negative feedback due to platform motions (particularly in pitch, with typical natural periods 30-40 s, and in surge, with typical natural periods 80-150 s) (Larsen and Hanson, 2007). Negative feedback occurs in above-rated wind speeds when the blade pitch control reacts to changes in the rotor speed in-phase with the in-line horizontal velocity of the rotor-nacelle-assembly (RNA). Effectively, a land-based wind turbine controller reacts faster than the typical rigid body motions of floating wind turbines. Several strategies to avoid this negative feedback have been proposed, among them:

- De-tuning: numerous academic studies simply modify K_I and K_P such that the controller is slower than the platform pitch (Nielsen et al., 2006; Jonkman, 2010).
- Nacelle velocity feedback: the measured horizontal nacelle velocity $\dot{x}_{RNA}$ can be fed back to the blade pitch controller, such that the commanded blade pitch becomes

$$\Delta\theta = K_P \Delta\omega + K_I \int_0^t \Delta\omega(\tau) d\tau + K_{fb}\dot{x}_{RNA} \tag{7}$$

where K_{fb} is a feedback gain (Abbas et al., 2022).

- Nacelle velocity feedforward: in this case, the nacelle velocity is used to modify the reference rotor speed, i.e.
$$\omega_{ref} = \omega_r + K_{ff}\dot{x}_{RNA} \quad (8)$$
where K_{ff} is a feedforward gain (de Souza and Bachynski-Polić, 2022).

While detuning is a simple way to obtain stability in platform pitch, it results in poor power tracking performance and large oscillations in rotor speed. Surge motions may still have negative feedback, but other sources of damping may be sufficient to maintain acceptable performance in surge. The last two approaches offer the advantage of maintaining a higher control frequency, but have tradeoffs in terms of allowed rotor speed variations.

3. UPSCALING OF FLOATING WIND TURBINES

Given the above control considerations for floating wind turbines, it is of interest to examine the effects of upscaling of the turbine. Traditional upscaling laws for wind turbines assume geometric upscaling of the rotor, unchanged incoming wind speed, and constant λ. Assuming a geometric ratio proportional to the rotor radius R and direct drive generator, one can easily see that how the power, rated speed, generator torque, mass and inertia scale (Table 1). Further assuming that the lift coefficient sensitivity to changes in the pitch angle remains unchanged by the scale, the scaling factor for $\frac{\partial P_{aero}}{\partial \theta}$ can also be found.

Table 1. Rotor upscaling

Power	P_{rated}	R^2
Rated speed	ω_{rated}	R^{-1}
Torque	Q	R^3
Mass	m	R^3
Inertia	I	R^5
Power sensitivity	$\frac{\partial P_{aero}}{\partial \theta}$	R^2

Based on Table 1, if one wants to maintain the same natural frequency and damping of the controlled rotor above rated wind speed, the magnitudes of K_I and K_P must increase significantly. Simultaneously, the maximum possible pitch rate typically decreases due to the large inertia of the blades.

Several possible scaling laws for the floating platform have been proposed. Geometric upscaling using the same scaling ratio as the rotor typically leads to an overdesigned platform, so alternatives have been proposed. One option is to scale based on the required increase in buoyancy based on the increase in rotor mass (Leimeister et al., 2016). One might alternatively maintain a constant draft, and scale the horizontal dimensions such that the mean platform pitch at rated wind speed remains constant. Of course, thrust clipping, which becomes increasingly important for larger turbines, would also affect the second option.

Although it is not possible to easily define a clear scaling law, the most important trend for the control design is to recognize that a well-designed upscaled platform will typically have a longer pitch natural period than the original platform. As a result - assuming that the goals of control for the single turbine remain unchanged - simple detuning becomes less attractive because the controller would be increasingly unable to track the desired output power. Nonetheless, the VolturnUS-S design for the IEA 15 MW reference turbine applies a combination of detuning and nacelle velocity feedback (Allen et al., 2021). One could alternatively argue for allowing larger power excursions in larger wind farms, assuming that the variations at the individual turbine level might average out over the entire farm.

4. PLATFORM PITCH PERIOD SCALING TREND

In this section, the variation of the pitch natural period of FWTs substructures with rotor power rating is illustrated by scaling the semi-submersible platform and floating tower of the reference FWT VolturnUS-S (Allen et al., 2021) to support 6 different rotors with power ratings ranging from 5 to 30 MW. The rotors used for this study are the NREL 5MW (Jonkman et al., 2009), the IEA 10MW (Bortolotti et al., 2019), the IEA 15MW (Gaertner et al., 2020), and three theoretically upscaled versions of the IEA 15MW rotor with power ratings of 20, 25, and 30 MW. Scaling the platform was achieved using a parametric study of the platform's geometry based on a simplified 2D model of FWTs. An illustration of the simplified model is given in Fig. 2 which shows the floating system idealized as a 2D finite element model considering only the surge, heave, and pitch motions of the platform and the first fore-aft tower bending mode. The static pitch under maximum thrust and the natural periods of rigid platform motions and tower bending modes are estimated from the simplified model. The substructure's geometry is selected by searching through the design space of different geometries of the platform for the design with minimum steel mass that satisfies the following requirements:

- Maximum static pitch of 6 degrees
- Minimum rigid body natural periods of 20 s
- Stiff-stiff floating tower (soft-stiff for the 5 MW design)
- Maximum hull horizontal dimension of 120 m

The towers used in this study are theoretically scaled versions of the floating tower of the VolturnUS-S FWT (the thickness and diameter increase proportional to the rotor radius). For the 10 MW design, a 20% increase in the tower thicknesses was implemented to achieve the stiff-stiff tower requirement.

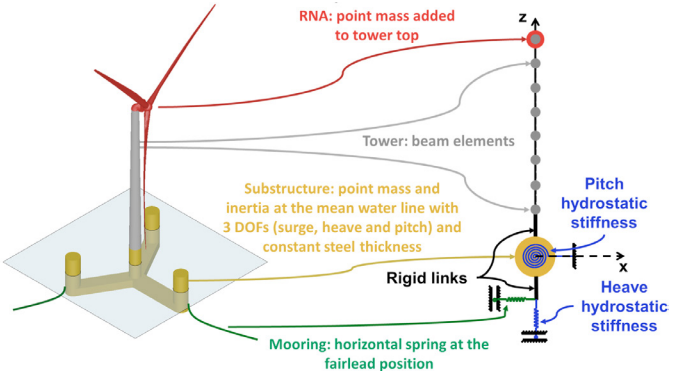

Fig. 2. Simplified 2D model for FWTs

Fig. 3 shows the variation of the natural periods of platform pitch and first tower fore-aft bending mode as a

function of rotor diameter. As expected, for a platform that satisfies basic requirements for a FWT, the pitch natural period increases as the rotor diameter increases. Moreover, the change in pitch natural period was found to be nearly proportional to the change in rotor diameter. Consequently, detuning the blade pitch controller to have a bandwidth that is less than the pitch natural frequency will result in increasingly slower controllers for larger rotor sizes. On the other hand, as the rotor diameter increases, the tower first fore-aft period moves further away from the range of operation of the blade passing period. This suggests that for FWTs with stiff-stiff towers, the excitation of the first tower mode becomes less vulnerable to variations in rotor speed as the turbine size increases.

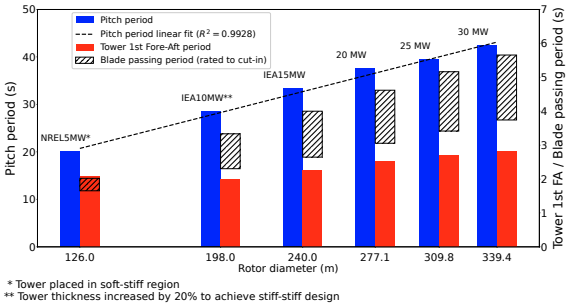

Fig. 3. Platform pitch and first tower fore-aft natural periods scaling trend

5. CASE STUDY: PITCH CONTROLLER OF 5, 15 AND 25 MW WIND TURBINES

Three wind turbines and their respective platforms have been compared considering a joint approach with detuned controllers and floating specific feedback. Simulations using OpenFAST were performed for the NREL 5 MW (Jonkman et al., 2009), IEA 15 MW (Gaertner et al., 2020), and a 25 MW wind turbine upscaled from the IEA 15 MW. The ROSCO controller (NREL, 2021) has been applied in all the cases. The desired damping ratio of the pitch controllers was defined as $\zeta_\psi = 1.0$ and the desired natural frequency as $\omega_{0,\psi} = 0.9\omega_{pit}$, where ω_{pit} is the pitch natural frequency of the platform. The desired damping ratio and natural frequencies of the torque controller are, respectively, $\zeta_\tau = 0.85$ and $\omega_{0,\tau} = 0.12$ rad/s (Abbas et al., 2022). Peak shaving of 80% has been applied with respect to the maximum thrust force. Fig. 4 compares the variation of the rotational speed with the rated rotational speed when the wind turbine experiences the same wind gust around $V_{ref} = 12$ m/s during 10.5 s based on the IEC 61400-1 extreme operating gust. Cases with and without the pitch controller have been analyzed. In this first analysis, the platform degrees of freedom were ignored, thereby emulating the behavior of bottom-fixed turbines.

The comparison in Fig. 4 reveals that despite upscale effects inherent to wind turbines from 5 to 25 MW, the rotor dynamics are similar when the blade pitch controller is not active. In this case, the rotational speed of the wind turbine slowly decays until reaching its rated value. On the other hand, the closed-loop with the controller modifies the system dynamics and the rated rotational

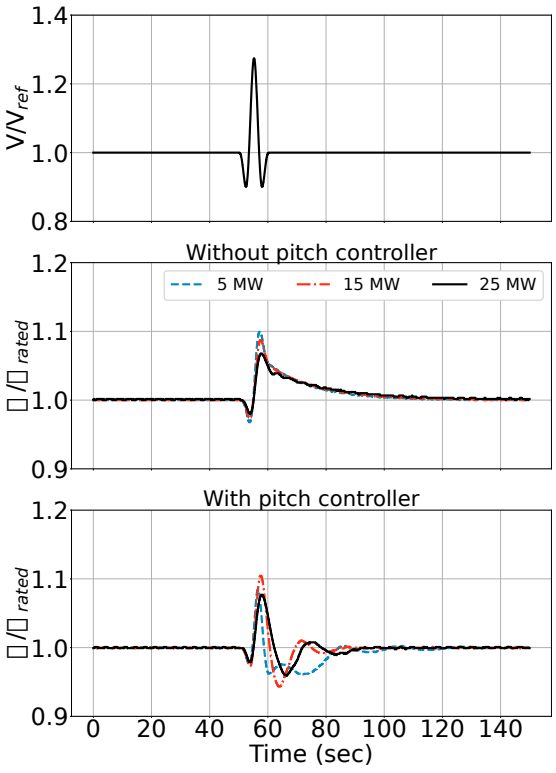

Fig. 4. Variation of the rotational speed during a wind gust

speed is reached 30% to 40% faster than the case without active pitching controller. Fig. 4 also highlights different frequency of oscillations for the different rotor sizes with the closed-loop controller.

When platform degrees of freedom are taken into account, the rotor speed shows an oscillatory behavior in above-rated conditions. Notwithstanding the nacelle velocity feedback implemented in ROSCO, the oscillatory behavior of the rotor speed is closely related to the platform behavior, as shown in Fig. 5. This result agrees with the findings in previous works (Larsen and Hanson, 2007; de Souza and Bachynski-Polić, 2022). Pitching and surging oscillations during step changes in the wind speed in the interval between 6 and 18 m/s have higher amplitudes as the rated power of the turbine increases. Such oscillations are not relevant in the case of the NREL 5 MW. Large oscillations with frequency around 0.01 Hz are observed in the interval of wind speeds between 12 and 14 m/s in the case of the IEA 15 MW, and become even divergent in the case of the 25 MW wind turbine at wind speeds around 12 m/s.

Therefore, at $V_{ref} = 12$ m/s (in region 3) the pitch controller requires special attention due to the possibility of negative feedback effects. In that sense, optimum parameters (ζ_ψ and $\omega_{0,\psi}$) can be sought to the ROSCO controller. Based on the performance index discussed by Ebrahim et al. (2018), the following optimization problem can be established:

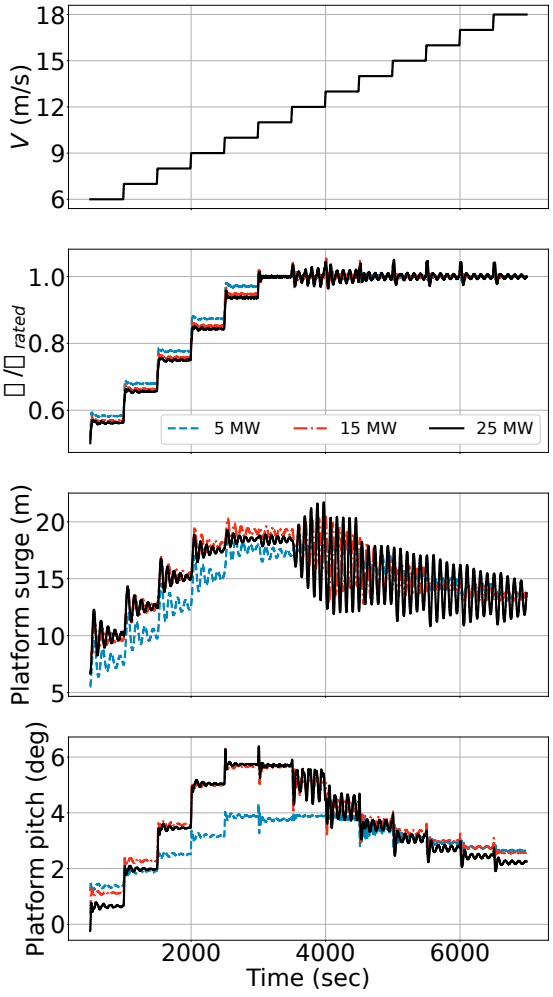

Fig. 5. Step wind response of the controller for different wind turbines (uniform wind)

$$\min_{(\zeta_\psi,\omega_{0,\psi})} \frac{1}{t_f}\int_0^{t_f} [P(t) - P_{rated}]^2 \, \mathrm{d}t \quad , \tag{9}$$

subject to:

$$\begin{cases} 0.1 \leq \zeta_\psi \leq 5.0 \\ 0.01 \leq \omega_{0,\psi} \leq 1 \end{cases} \quad . \tag{10}$$

The optimization problem is constrained for feasible solutions and can be solved through the SQP method (Rao, 2009). In the case of the 25 MW wind turbine, the optimum condition was reached when $\zeta_\psi = 2.018$ and $\omega_{0,\psi} = 0.0709$ rad/s. Fig. 6 shows the performance of the 25 MW considering the same parameters as before, and the optimized parameters of the pitch controller. Turbulent wind around $V_{ref} = 12$ m/s is employed during the analyzes. The rotor speed is very similar for both controllers. On the other hand, a relevant difference is observed in the platform dynamics: the use of optimum parameters for the pitching controller reduces up to 60% the amplitude of surging and pitching oscillations of the platform.

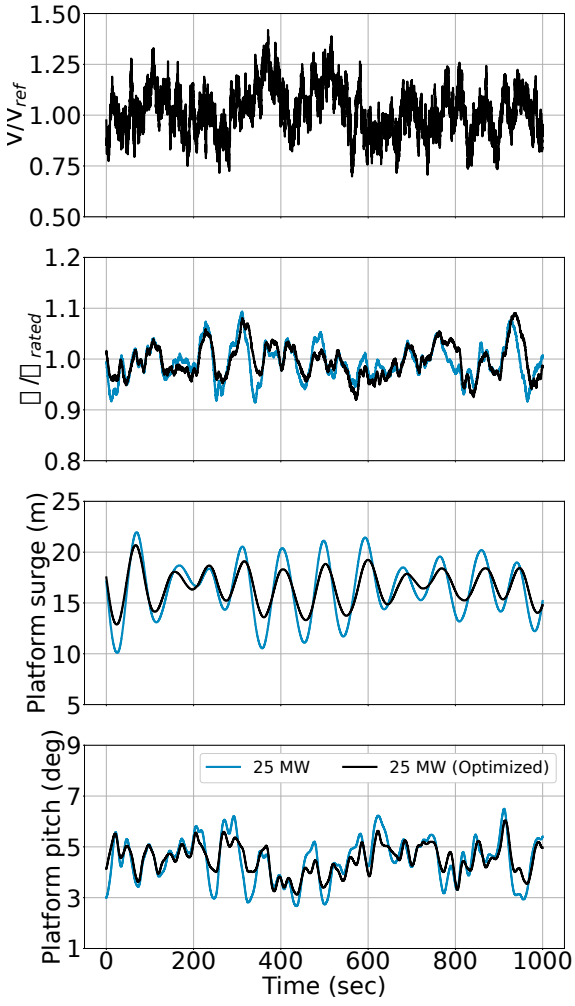

Fig. 6. Effects of optimization parameters on turbine performance under turbulent wind conditions

6. CONCLUSION

This work sheds light on relevant aspects concerning the design of controllers for very large floating wind turbines. As the rotor size increases, the natural pitch period of the floating platform also increases, thereby leading to slower controllers when applying detuning. Such an approach leads to controllers whose dynamic response includes limit cycle oscillations and even instabilities at wind speeds near rated conditions. The use of optimum parameters for the controller can reduce the amplitude of these oscillations. In future steps of this work, other control strategies, such as the nacelle velocity feed-forward, are going to be investigated for their capabilities of improving the power

quality and reducing structural loads. Numerical models will also be applied to understand better the coupling between the motions of the platform and the turbine itself.

ACKNOWLEDGEMENTS

The research leading to these results has received funding from the Research Council of Norway through the ENERGIX program (grant 308839) and industry partners Equinor, AIBEL, Dr. Techn. Olav Olsen, GCE Node Service, and Energy Valley.

REFERENCES

Abbas, N.J., Zalkind, D.S., Pao, L., and Wright, A. (2022). A reference open-source controller for fixed and floating offshore wind turbines. 7(1), 53–73. doi:10.5194/wes-7-53-2022. URL https://wes.copernicus.org/articles/7/53/2022/.

Allen, C., Viselli, A., Daghree, H., Goupee, A., Gaertner, E., Abbas, N., Hall, M., and Barter, G. (2021). Definition of the UMaine VolturnUS-S reference platform developed for the IEA Wind 15-Megawatt offshore reference wind turbine. Technical report, National Renewable Energy Laboratory.

Bak, C., Zahle, F., Bitsche, R., Kim, T., Yde, A., Henriksen, L., Andersen, P., Natarajan, A., and Hansen, M. (2015). Description of the DTU 10 MW reference wind turbine.

Bortolotti, P., Tarrés, H.C., Dykes, K., Merz, K., Sethuraman, L., Verelst, D., and Zahle, F. (2019). Systems engineering in wind energy-wp2. 1 reference wind turbines. Technical report, Technical Report No. NREL/TP-5000-73492, National Renewable Energy ....

Bossanyi, E.A. (2003). Wind turbine control for load reduction. 229–244. doi:10.1002/we.95.

de Souza, C.E.S. and Bachynski-Polić, E.E. (2022). Design, structural modeling, control, and performance of 20 MW spar floating wind turbines. 84, 103182. doi: https://doi.org/10.1016/j.marstruc.2022.103182.

de Souza, C.E.S., Berthelsen, P.A., Eliassen, L., Bachynski, E.E., Engebretsen, E., and Haslum, H. (2021). Definition of the INO WINDMOOR 12 MW base case floating wind turbine. Technical Report OC2020 A-044, SINTEF Ocean AS.

Ebrahim, M.A., Becherif, M., and Abdelaziz, A.Y. (2018). Dynamic performance enhancement for wind energy conversion system using moth-flame optimization based blade pitch controller. *Sustainable Energy Technologies and Assessments*, 27, 206–212.

Gaertner, E., Rinker, J., Sethuraman, L., Zahle, F., Anderson, B., Barter, G., Abbas, N., Meng, F., Bortolotti, P., Skrzypinski, W., Scott, G., Feil, R., Bredmose, H., K, D., Shields, M., Allen, C., and Viselli, A. (2020). Definition of the IEA 15-Megawatt offshore reference wind turbine.

Gottschall, J., Gribben, B., Stein, D., and Würth, I. (2017). Floating lidar as an advanced offshore wind speed measurement technique: current technology status and gap analysis in regard to full maturity. *Wiley Interdisciplinary Reviews: Energy and Environment*, 6(5), e250.

Ha, K., Truong, H.V.A., Dang, T.D., and Ahn, K.K. (2021). Recent control technologies for floating offshore wind energy system: A review. *International Journal of Precision Engineering and Manufacturing-Green Technology*, 8(1), 281–301.

Jonkman, J., Butterfield, S., Musial, W., and Scott, G. (2009). Definition of a 5-MW reference wind turbine for offshore system development. Technical Report NREL/TP-500-38060, National Renewable Energy Laboratory.

Jonkman, J. (2010). Definition of the floating system for Phase IV of OC3. Technical Report NREL/TLP-500-47535.

Larsen, T.J. and Hanson, T.D. (2007). A method to avoid negative damped low frequent tower vibrations for a floating, pitch controlled wind turbine. *Journal of Physics: Conference Series, The Second Conference on The Science of Making Torque from Wind*, 75.

Leimeister, M., Bachynski, E.E., Muskulus, M., and Thomas, P. (2016). Rational upscaling of a semi-submersible floating platform supporting a wind turbine. *Energy Procedia*, 94, 434–442. doi: 10.1016/j.egypro.2016.09.212.

Manwell, J., McGowan, J.G., and Rogers, A.L. (2009). *Wind Energy Explained*. John Wiley & Sons, Ltd.

Nielsen, F.G., Hanson, T.D., and Skaare, B. (2006). Integrated dynamic analysis of floating offshore wind turbines. In *25th International Conference on Ocean, Offshore, and Arctic Engineering*, OMAE2009-79229.

NREL (2021). ROSCO. Version 2.3.0. URL https://github.com/NREL/ROSCO.

Rao, S.S. (2009). *Engineering optimization*. John Wiley, New York.

Salic, T., Charpentier, J.F., Benbouzid, M., and Le Boulluec, M. (2019). Control strategies for floating offshore wind turbine: challenges and trends. *Electronics*, 8(10), 1185.